Proceedings, 7th African Rift Geothermal Conference
Kigali, Rwanda 31st October – 2nd November 2018

Mapping of hydrothermal alteration of the Lake Natron – Oldoinyo Lengai geothermal area in Northern Tanzania using satellite imagery

[1,4]Albano Mahecha, [2]Nureddin Saadi, [2]KotaroYonezu, [1,2]Koichiro Watanabe, [3]Jacob Mayalla

[1]Corporative Program for Sustainable Resource Engineering, Kyushu University, Japan
[2]Department of Earth Resource Engineering, Kyushu University, Japan
[3]Ministry of Energy, Dodoma, Tanzania
[4]Tanzania Geothermal Development Company Limited, Dar es Salaam, Tanzania

Albano@mine.kyushu-u.ac.jp

Keywords

Hydrothermal alteration, PCA, Natron, OLI Sensor

ABSTRACT

The Lake Natron- Oldoinyo Lengai geothermal area is confined to Natron- Manyara rift, part of the East Africa Rift System in northern Tanzania and characterized by Pliocene through Pleistocene to the recent volcanic events.

The area has numerous geothermal manifestations which to large extent remain poorly studied in geothermal resource potential context. The image processing methods; false colour band composite (FCC) and Principal Component Analysis (PCA) transformation are applied to satellite imagery data acquired from OLI sensor to assess the surface hydrothermal alterations for characterizing the hydrothermal water-rock interaction. The alteration zones vindicate the relationship between the hydrothermal fluid flow and structures. The types of alteration suggest an influence of carbonatite from the Oldoinyo Lengai especially on the southern and southwestern part of the area. Among other scientific analysis, hydrothermal alteration mapping can be used as a tool for evaluating the characteristics of the geothermal systems. Alteration mapping in the area has highlighted the relationship between the structure, permeability and hydrothermal fluid flow. The presence of trona and Na $–CO_3$-type water argued to be contributed by magmatic CO_2 suggests that there is substantial permeability to allow the geothermal fluid flow. The type of alteration suggests an influence of carbonatite volcano from the Oldoinyo Lengai especially on the southern and southwestern part of the area.

1. Introduction

The remote sensing imagery data has long been applied over a number of applications in geosciences studies (Calvin et al, 2015). The application ranges from mineral, geothermal exploration to volcanic activity monitoring. In geothermal and volcanology studies, remote sensing imagery is widely applied in a mapping of geological structures, volcanic eruptive centre, thermal anomaly or surface temperature distribution, and hydrothermal alterations (Calvin et al., 2015; Mia & Fujimitsu, 2013; Ulusoy, 2016)

In this paper, satellite imagery data acquired from OLI sensor are applied in mapping the hydrothermal alteration and thermal anomaly associated with a geothermal resource in Lake Natron – Oldoinyo Lengai area in Arusha region, Northern Tanzania. Remote sensing can be vital in unlocking, locating and assessing the geothermal resources with surface manifestation and those considered to be blind systems with no clear surface expression. The hydrothermal alteration assessed in this study is to evaluate the characteristics of a geothermal system in the area and being able to identify the structures associated with the geothermal resource in Natron-Oldoinyo Lengai area. This area is characterized by numerous hot springs and active volcano i.e. Oldoinyo Lengai volcano.

The Natron- Oldoinyo Lengai geothermal area is located within the Natron- Manyara rift, which makes part of the East Africa rift system in Northern Tanzania bordering Kenya.

2. Geology and Tectonic Setting

The Great rift of East Africa (Fig. 1) is an approximately north-south trending structure system stretching from Gulf of Eden to Mozambique(Dawson, 2008). It is made up of two branches; the eastern arm which is referred as Gregory rift and the western arm referred as Albertine rift. The eastern arm stretches from Gulf of Eden through Ethiopia and Kenya to northern Tanzania where it splits into two major armed rift patterns (Dawson, 2008). The NE - SW trending tilted fault blocks south of Lake Natron, which occupy Eyasi rift and Manyara rift. To the East the Monduli, Meru and Kilimanjaro volcanoes (trending WSW - ENE) are located within the Kilimanjaro depression (Le Gall et al., 2008) which connect to the NNW - SSE trending Pangani fault system. This rift split is referred as Northern Tanzania Divergence (Le Gall et al., 2008). The rift then continues to central Tanzania Archean craton, at this point the rift is not as continuous as prior to the Northern Tanzania Divergence. The rift stretches further south to the triple junction where it intersect the Albertine rift.

The structure of this elongated north – south rift is dominated by Ethiopian and Kenya domal uplift on which geological studies and geochronological examinations have shown to have developed simultaneously with the rift system during Cenozoic faulting and volcanism (Fairhead, 1980)

The Neogene volcanic region of northern Tanzania divergence is recognized to be younger than the volcanic provinces in Kenya and Ethiopia where magmatism was initiated around 40Ma (Dawson, 2008) which suggest that further mantle uprising is accountable for intra-plate magmatism and crustal fracturing in this province (Dawson, 2008). The province is underlain by Precambrian basement and bordered by Precambrian metamorphic rocks to the east and Archean craton rocks of Central and Northern Tanzania to the west.

The region is dominated by Neogene to recent volcanics erupted within the rift system. The major volcanoes in the region include the late tertiary to early Pleistocene volcanoes. Tertiary

volcanics include the Shombole, Oldoinyo sambu, Masonik, Gelai, Olmoti, Ketumbeine, Tarosero, Elanairobi, Lemaguruti, Essimingor, Oldean and Kilimanjaro (Kibo, Shira and Mawenzi peak). Upper pleistocene to recent volcanoes are namely; Oldoinyo Lengai, Meru, Kerimasi, Sadiman, Burko and Monduli (Dawson, 1962; Wilkinson, Mitchell, Cattermole, & Downie, 1986) . Previous geological studies confirm that the major rift faulting episodes in the northern Tanzania to be around 2.1Ma and 1.2Ma (Wilkinson et al., 1986), while Foster et al (1997) argued that the existing rift escarpments evolved later than *c.* 1.2 Ma and major fault escarpments were exist by *c.* 3 Ma. The petrology of the volcanoes is heterogeneous ranging from basalt-trachyte-phonolite to nephelinite-phonolite associations (Fairhead, 1980).

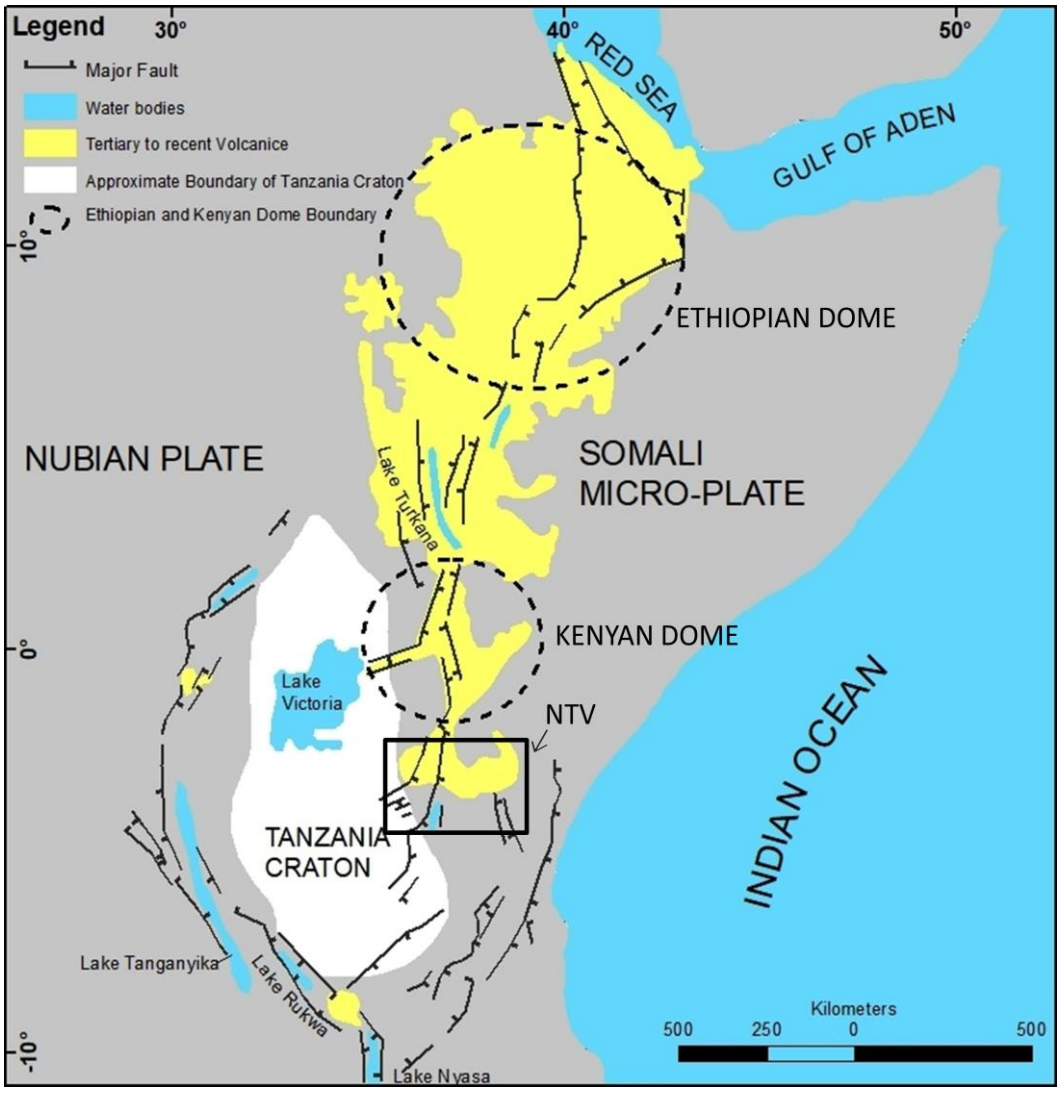

Figure 1: The East Africa tectonic map showing the extent of the East Africa rift system and volcanic province. NTV (Northern Tanzania Divergence), Ethiopian and Kenyan domes are highlighted (edited from Dawson, 2008).

2.1 Geothermal Manifestation

Volcanic regions and regions in active tectonic activity, thus areas in and/or proximal to divergence or convergent boundaries have long been the target for geothermal exploration. The exploration of geothermal resources is traditionally guided by the surface expression resulted from the presence of a heat source beneath the earth's surface. Thermal

manifestations of a convectional geothermal system can visually be identified on the surface in a respective area of interest. Common surface manifestations are fumaroles, hot springs, hot ground, hydrothermal alteration, mud pot, geysers and Solfatara.

Lake Natron-Oldoinyo Lengai area is characterized by active volcanic activity, specifically the boiling lava at the vents on top of Oldoinyo Lengai volcano. The other geothermal manifestation in the region are discussed below

2.1.1. Hot springs

One set of the thermal spring are observed on the western flank of the rift, which is also the south western end of the Lake Natron. The springs emanates from fractures on the basaltic rock flowing towards the lake. The temperature ranges from 48 ºC to 56 ºC and the measured minimum water temperature of some rivers flowing towards the lake from the southern part of the area was 27 ºC, (measured during the field work) which is a bit higher compared to other rivers in the region

The other set of thermal spring are located on the eastern boundary of Lake Natron which coincides with the western flank end of the Gelai volcano. The temperatures of the springs on this side are generally lower than of the western side of the Lake. The temperature ranges between 35 ºC and 50 ºC

2.1.2. Fumaroles

The fumaroles are constrained on the northern flank of the Oldoinyo Lengai volcano facing towards lake Natron. There were three fumarolic activity point observed during the fieldwork. According to locals, the mountain climbers' guide, two of the three fumaroles are new and were observed sometime in 2016. The temperature of the fumaroles was not measured during the field work.

3. Materials and Methods

3.1 Remote sensing data

Landsat 8 imagery and the digital elevation model derived from SRTM (Shuttle Radar Topography Model) data of 90m pixel resolution are used in analysis. Landsat 8 (L8) is a new product launched on February 2013, in a continuous series of land remote sensing satellites that began in 1972, operated by National Aeronautics and Space administration (NASA) and United States Geological Survey (USGS). Landsat 8 has a total of 11 channels and carries two sensor payload; Operational Land Imager (OLI) and Thermal Infrared Sensor (TIRS). OLI sensor has 9 spectral bands (band 1 through band 9) while 2 thermal infrared bands (Band 10 and 11) are for TIRS. The image was downloaded from USGS website and freely available, captured on 13th October, 2016.

Table 1: Landsat 8 OLI/TIRS bands (µm)

Band 1	30 m Coastal/Aerosol	0.435 – 0.451
Band 2	30 m Blue	0.452 – 0.512
Band 3	30 m Green	0.533 – 0.590
Band 4	30 m Red	0.636 – 0.673
Band 5	30 m NIR	0.851 – 0.879
Band 6	30 M SWIR-1	1.566 – 1.651
Band 7	30 m SWIR-2	2.107 – 2.294
Band 8	15 m Pan	0.503 – 0.676

Band 9	30 m Cirrus	1.363 – 1.384
Band 10	100m TIR-1	10.60 – 11.19
Band 11	100m TIR- 2	11.50 – 12.51

3.2 Field reconnaissance

A field survey was conducted on the study area to verify the observation from the remote sensing. The idea was to get the representative altered and fresh rock samples for laboratory analysis. Representative rock samples and photographs of thermal manifestation and altered samples were taken during the field work for the X-Ray Diffraction analysis. Location coordinates were recorded using Garmin 64S GPS. Physical parameters of the hot spring were measured and recorded.

4. Image Analysis

4.1 Data Preprocessing

Atmospheric correction was done on the imagery to get the surface reflectance as the final product by applying FLAASH algorithm using ENVI software and then followed by data resizing to focus on the area of interest.

4.2 Image processing technique

The image processing methods used in this analysis are false color band combination (FCC) and Principle Component Analysis (PCA); whereby in FCC analysis, spectral bands are composited in Red Green and Blue color combination to highlight specific observation (figure 2) while PCA is a multivariate statistical technique which selects uncorrelated linear combinations (eigenvector loadings) of variables in such a way that each successively extracted linear combination, or principal component (PC), has a smaller variance. The statistical variance in multispectral images correspond to the spectral response of various surface materials such as rocks, soils, and vegetation, and it is also controlled by the statistical dimensionality of the image data (Loughlin, 1991; Singh & Harrison, 1985). The algorithm (Richards, 1995) can be defined as:

$$y = G \# x \quad (1)$$

Where:

y = The transformed, or rotated data (i.e., the principal components data),

$\boldsymbol{G}$ = The transformation matrix,

x = The original data,

refers to matrix multiplication.

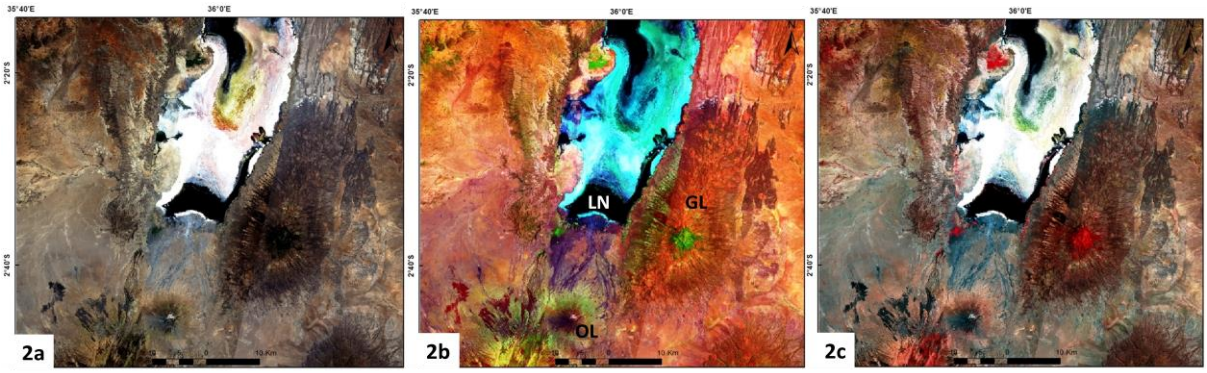

Figure 2: True color composite of the study area: RGB 432 (2a), false color image, RGB 753 highlighting solid surface- soil and rocks in brown and red, vegetation in green, water in black, carbonates in white and evaporates in greenish bright color (2b), false color image, RGB 543 highlighting intensity of vegetation in red color. OL=Oldoinyo Lengai Volcano, LN=Lake Natron and GL=Gelai volcano

Crosta Technique

The method is based on the evaluation of PCA eigenvector loadings to decide which of the principal component images will concentrate information directly related to the theoretical spectral signatures of specific targets. The approach is that it predicts whether the target surface type is highlighted by either dark or bright pixels in the relevant principal component image. This method specifically relies on the selective input of only four image bands for PCA.

The target bands in these eigenvector are band 2 and 4 in opposite sign (negative which means absorption and positive means reflectance) which are highlighting iron oxide minerals. Iron oxide minerals have high reflectance on band 4 and high absorption in band 2 and 3 wavelengths. On the other hand band 6 and 7 will be used to highlight hydroxyl bearing and clay minerals which tend to have high absorption at band 7 and high reflectance at band 6.

Table 2 shows eigenvector loadings for principle component transformation of six bands namely; 2, 3,4,5,6 and 7. This transformation has been carried out in raw data. PC1, PC2 and PC 3 are highlighting the albedo information, vegetation and difference between the visible channels (2, 3, 4) and other infrared channels (5,6,and 7) respectively. The remaining three PCs are expected to contain information due to the varying spectral response of iron-oxides and hydroxyl-bearing minerals (Loughin, 1990: Bands 1,2,3 and 4,5,7 of TM bands are equivalent of band 2,3,4 and 5,6,7 of Landsat 8 respectively). Band 2 and 4 or band 6 and 7 are checked against each other to see if they contain eigenvalue in opposite signs i.e. positive or negative which reflect reflection or absorption respectively, based on mineral characteristics in response to radiation.

Table 2: Principal Component Analysis of six bands of Landsat 8 imagery

Eigenvector	Band 2	Band 3	Band 4	Band 5	Band 6	Band 7	Eigenvalue	
PC1	0.211512	0.287204	0.389242	0.482548	0.552779	0.42761	0.010938	57.88%
PC2	-0.32569	-0.3696	-0.41605	-0.30278	0.47247	0.518965	0.007287	38.56%
PC3	-0.3452	-0.30236	-0.2533	0.669572	0.2438	-0.46636	0.000429	2.27%
PC4	-0.46896	-0.18833	0.263171	0.324268	-0.57223	0.4927	0.00019	1.01%

PC5	-0.56496	0.036838	0.624006	-0.34781	0.288185	-0.29335	0.000041	0.22%
PC6	-0.43695	0.807874	-0.39063	0.031981	-0.03565	0.039098	0.000012	0.06%

The eigenvector loadings of Table 3 have been used to map iron oxide minerals. PCs of band 2, 4, 5 and 6 have been analysed. Band 2 and 4 eigenvector loadings are checked to see the existence of loading in opposite signs i.e. positive or negative. PC4 image of Table 3 shown in (Fig. 3a) highlight the iron oxide (F image) in dark pixels instead of bright pixel; represented by positive sign in band 2 means high reflectance where as negative sign in band 4- means absorption, which is opposite representation of a characteristic of iron oxide minerals in band wavelengths.

PC4 image (H image) of Table 4 represents the hydroxyl bearing minerals e.g. clay, in dark pixel (Figure 3b). From theoretical understanding, hydroxyl bearing minerals have high absorption in band 7 (negative loading) and high reflectance in band 6 (positive loading). In this case it is a vice versa representation such that hydroxyl bearing is highlighted by dark pixel instead of bright pixel. Band 4 in Table 4 is ignored to avoid mapping of oxide minerals. PC3 of Table 4 mapped hydroxyl bearing minerals where band 7 (negative) shows absorption and band 6 (positive) shows reflectance, typical of hydroxyl mineral characteristic but the loading contribution of band 6 and 7 is lower than in PC4.

Table 3: Principle Component analysis of band 2, 4, 5 and 6

Eigenvector	**Band 2**	**Band 4**	**Band 5**	**Band 6**	**Eigenvalue**	
PC1	0.304175	0.521837	0.612702	0.509667	0.008345	64.99%
PC2	0.336534	0.394621	0.19022	-0.83357	0.004145	32.28%
PC3	0.589815	0.294667	-0.72103	0.213084	0.000278	2.17%
PC4	0.668087	-0.69651	0.261777	-0.00028	0.000072	0.56%

Table 4: Principle component analysis of band 2, 5, 6 and 7

Eigenvector	**Band 2**	**Band 5**	**Band 6**	**Band 7**	**Eigenvalue**	
PC1	0.068971	0.338101	0.71319	0.610156	0.00963	68.94%
PC2	-0.54109	-0.76377	0.137063	0.324178	0.003875	27.74%
PC3	-0.75863	0.396641	0.264993	-0.44377	0.000293	2.10%
PC4	-0.3563	0.38081	-0.63431	0.570686	0.000171	1.22%

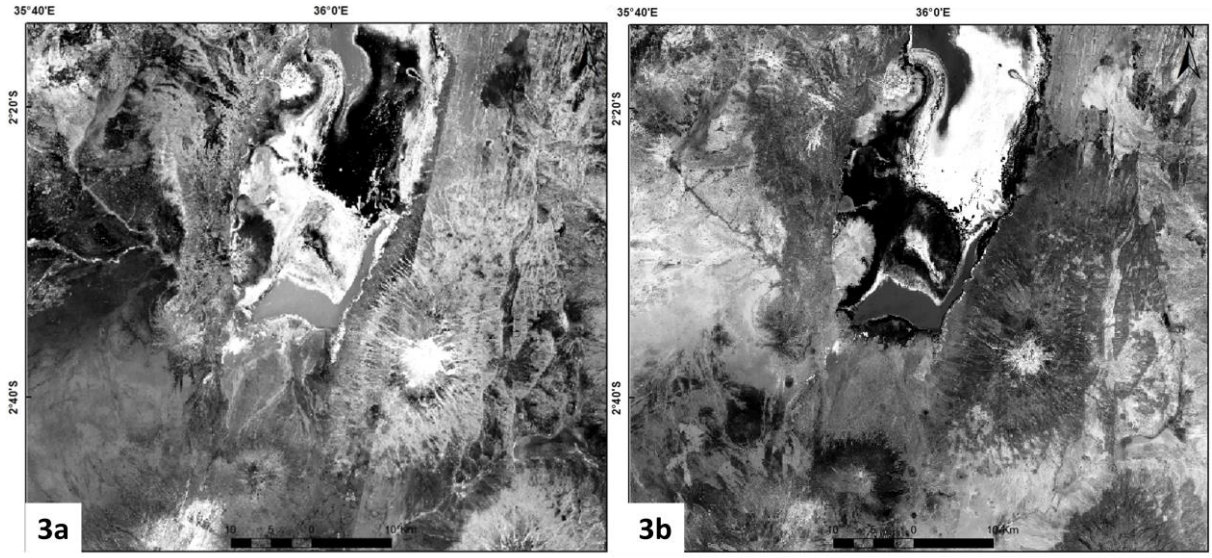

Figure 3: PC4 image of band 2, 4, 5 and 6 referred as F image (3a) and PC4 image of band 2, 5, 6 and 7 referred as H image (3b)

6. Results and Discussion

Based on Crosta method technique, Hydroxyl image (H image) and Iron oxide image (F image) were added to produce a third image; (H+F) image that together with H and F image have been used to create a false color composite (FCC) image in RGB (R=Red, G= Green, B=Blue) which is highlighting the area of hydrothermal alterations (Fig. 4).

The result shows that most part of the lake is dominated by evaporates, most notably the trona which occupies western and eastern edges of the lake. This coincides with locations of hot springs emanating from the lake boundaries and which are feeding the lake (Fig. 4). Patches of clay minerals (deep blue) are seen on the lower slopes of Oldoinyo Lengai and nearby areas and also in the North Eastern part of the map. Iron oxide bearing minerals dominate the northern half of the lake, probably associated with carbonates, also on the western and eastern part of the study area, covering north and east of Gelai volcano. White colour on the map has been interpreted as carbonates probably with slight difference in composition with evaporates, which is seen on top of Oldoinyo Lengai and around the lake area.

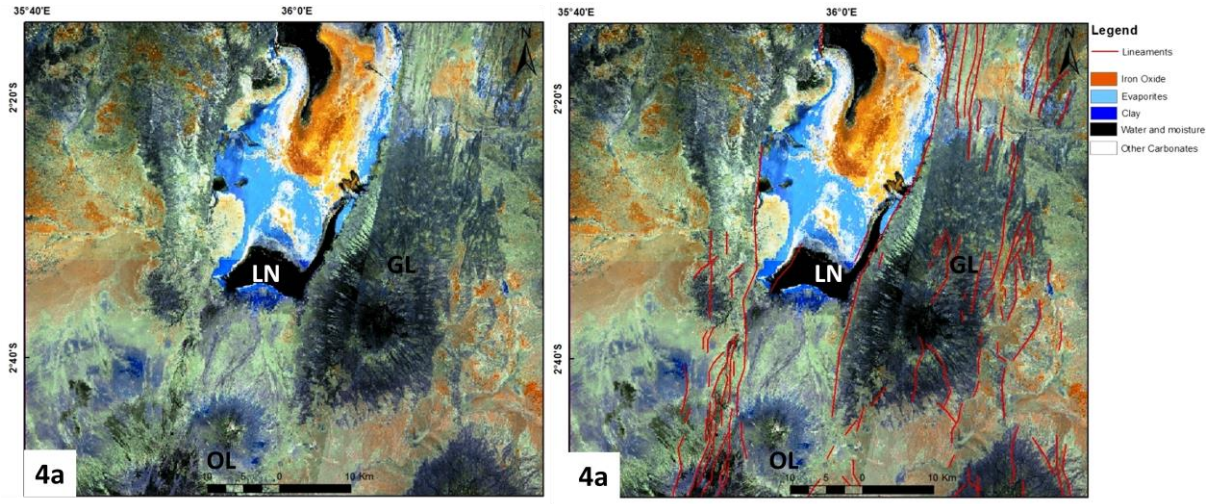

Figure 4: The image showing patches of alteration mapped after compositing of H , H+F and F images in RGB (4a) ; Lineaments extracted from SRTM data overlaid on the alteration map to highlight its relationship with mapped altered areas (4b) i.e. hydroxyl and iron oxide bearing mineral. OL= Oldoinyo Lengai, LN= Lake Natron and GL= Gelai volcano.

The relationship between the structure and hydroxyl-bearing mineral is obvious. On the eastern area southwestern area, the interpreted altered areas are coinciding with the structure extracted, which suggest that the alterations are related to hydrothermal activity.

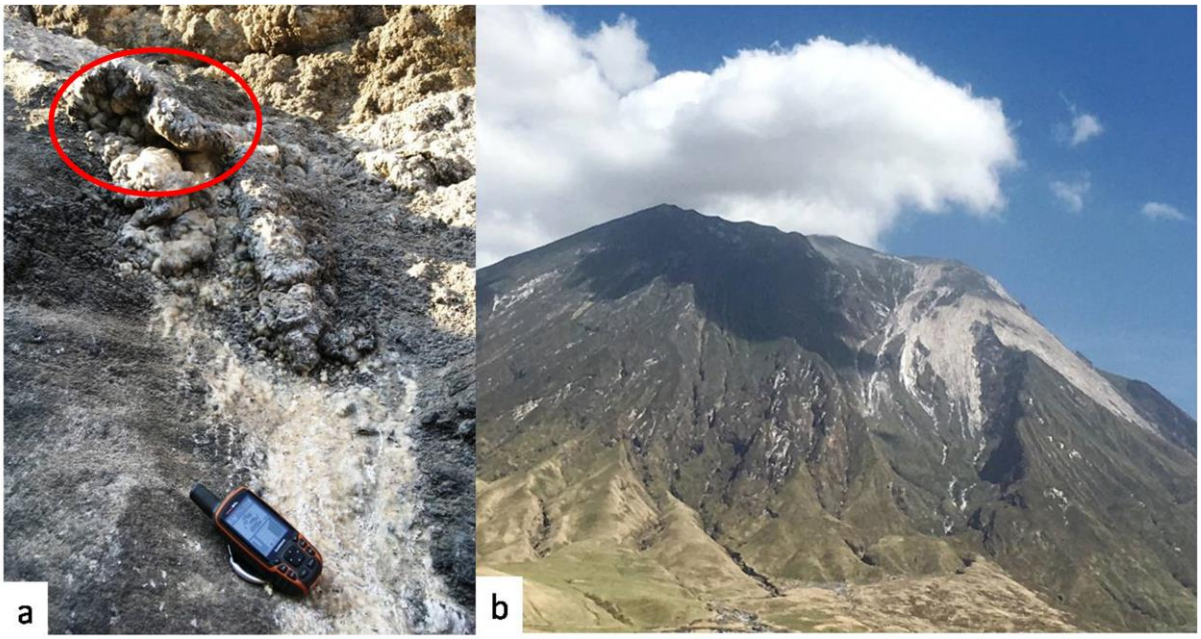

Figure 5: Hydrothermal precipitate from the small vent (highlighted with red circle) found at the lower northern slope of Oldoinyo Lengai (a); the picture of northern side of the Oldoinyo Lengai mountain showing the coverage of the precipitate mapped as hydroxyl alteration on remote sensing image

The precipitated sample was taken at a locality in Figure 5a, and the XRD result analysed in form of a bulk and oriented sample, shows strong peaks of trona and moderate mordenite and natroalunite. Mordenite is a zeolite group mineral and its genesis can be sedimentary or hydrothermal (Gottardi and Galli, 1985), with regard to the location of the sample it seems reasonable to assume that it has formed from hydrothermal processes and probably crystallized at low temperature.

It is suggested that most deposits of trona and Na–CO_3-type lakes revealed to have had substantial CO_2 input (Earman et al, 2005), which comes from either magmatic sources or the decay of organic matter. Results from this study are in agreement with the previous argument by Earman et al (2005) that CO_2 is an important pre-condition for the genesis of trona deposits. It is suggested that even at Lake Natron and surrounding area; the magmatic CO_2 has contributed to the formation of trona and evaporates deposition. This suggestion is in line with previous work by Muirhead et al. (2016) that there is high fluxes of magmatic CO_2 around Lake Natron. This suggests that the hydrothermal fluid is widely circulating and there is substantial permeability to allow the flow of fluid.

7. Conclusion

At the infant stage of geothermal exploration, remote sensing data is crucial in reducing the massive fieldwork and identifying a potential area of further investigation. Alteration mapping in this piece of work has highlighted the relationship between the structure, permeability and hydrothermal fluid flow. The presence of trona and Na –CO_3-type water argued to be contributed by magmatic CO_2 suggests that there is substantial permeability to allow the geothermal fluid flow. The type of alteration suggests an influence of carbonatite volcano from the Oldoinyo Lengai especially on the southern and southwestern part of the area. The alteration on the northern part of the area is possibly formed from a different source of the hydrothermal fluid as it is more associated with iron oxide than on the southern part and by considering the hydrological aspect on the area. Further geophysical work to identify potential geothermal reservoir on the eastern part, northern end of Gelai volcano and south western part of Lake Natron is recommended and isotopic analysis of water samples from the springs on the eastern part of the lake to understand the origin and geochemical signature of the water is also recommended.

REFERENCES

Calvin, W. M., Littlefield, E. F., & Kratt, C. (2015). Geothermics Remote sensing of geothermal-related minerals for resource exploration in Nevada. *Geothermics*, *53*, 517–526. https://doi.org/10.1016/j.geothermics.2014.09.002

Dawson, J. B. (1962). The geology of Oldoinyo Lengai. *Bulletin Volcanologique*, *24*(1), 349–387. https://doi.org/10.1007/BF02599356

Dawson, J. B. (2008). 'The Gregory Rift Valley and Neogene-Recent Volcanoes of Northern Tanzania'. *Geological Society, London, Memoirs* (Vol. 33). https://doi.org/10.1144/M33.0

Earman, S., Phillips, F. M., & McPherson, B. J. O. L. (2005). The role of "excess" CO2 in the formation of trona deposits. *Applied Geochemistry*, *20*(12), 2217–2232. https://doi.org/10.1016/j.apgeochem.2005.08.007

Fairhead, J. D. (1980). The structure of the cross-cutting volcanic chain of Northern Tanzania and its relation to the East African rift system. *Tectonophysics*, *65*(3–4), 193–208. https://doi.org/10.1016/0040-1951(80)90074-8

Gottardi G., & Galli E. (1985). Minerals and Rocks -Natural Zeolites.

Le Gall, B., Nonnotte, P., Rolet, J., Benoit, M., Guillou, H., Mousseau-Nonnotte, M., … Deverchère, J. (2008). Rift propagation at craton margin. Distribution of faulting and volcanism in the North Tanzanian Divergence (East Africa) during Neogene times. *Tectonophysics*, *448*(1–4), 1–19. https://doi.org/10.1016/j.tecto.2007.11.005

Loughlin, W. P. (1991). Principal Component Analysis for Alteration Mapping. *Photogrammetric Engineering & Remote Sensing*, *57*(9), 1163–1169.

Mia, M. B., & Fujimitsu, Y. (2013). Landsat Thermal Infrared based Monitoring of Heat Losses from Kuju Fumaroles Area in Japan. *Procedia Earth and Planetary Science*, *6*(2012), 114–120. https://doi.org/10.1016/j.proeps.2013.01.016

Muirhead, J. D., Kattenhorn, S. A., Lee, H., Mana, S., Turrin, B. D., Fischer, T. P., … Stamps, D. S. (2016). Evolution of upper crustal faulting assisted by magmatic volatile release during early-stage continental rift development in the East African Rift. *Geosphere*, *12*(6), 1670–1700. https://doi.org/10.1130/GES01375.1

Richards, J. A. (2005). *Remote Sensing Digital Image Analysis*.

Singh, A., & Harrison, A. (1985). Standardized principal components. *International Journal of Remote Sensing*, *6*(6), 883–896. https://doi.org/10.1080/01431168508948511

Ulusoy, İ. (2016). Temporal radiative heat flux estimation and alteration mapping of Tendürek volcano (eastern Turkey) using ASTER imagery. *Journal of Volcanology and Geothermal Research*, *327*, 40–54. https://doi.org/10.1016/j.jvolgeores.2016.06.027

Wilkinson, P., Mitchell, J. G., Cattermole, P. J., & Downie, C. (1986). Volcanic chronology of the Men-Kilimanjaro region, Northern Tanzania. *Journal of the Geological Society*, *143*(4), 601–605. https://doi.org/10.1144/gsjgs.143.4.0601